Modern Trends for Neutron Monitoring

Z.M. Badawy, Ahmed H.M. Solieman and M. Fayez-Hassan

Experimental Nuclear Physics Department, AEA, Egypt
Dr_zaynab_badawy@hotmail.com

Abstracts: This work represents a modern tool for neutron flux monitoring. The method based on the effect of the neutron field on the stress of the stainless steel materials. The neutron hardening effect on stainless steel foils were reported using the Vickers hardness test in air at room temperature. Am-Be neutron facility was used for the sample irradiation in thermal mode. The result was normalized with HPGe 70% detector using Indium foils as neutron flux monitoring. The method can be used successfully for different nuclear reaction laboratories.
[Z.M. Badawy, Ahmed H.M. Solieman and M. Fayez-Hassan. **Modern Trends for Neutron Monitoring.** *Nat Sci* 2013;11(5):119-125]. (ISSN: 1545-0740). http://www.sciencepub.net/nature. 18

Key words: Stainless-steel, neutron flux monitoring, NAA.

1.Introduction

Monitoring the neutron flux is very important for all activation experiments. The foil activation technique[1] has been found to be one of the most convenient methods for the measurement of neutron. Foil activation is widely used method to determine the neutron flux at different locations around the irradiation facility. This method is based on recovering information about neutrons by registering the products of induced reactions on selected materials[2]. However, this activation technique needs very elaborate and expensive gamma spectroscopy system for measurement of the produced photons of activated nuclei. In addition, it needs a cautious and tedious work for the analysis of gamma spectra. Therefore, measurement of mechanical properties of neutron sensitive materials[3] may provide an easier and less expensive method for flux monitoring.

This work aims to explore the suitability of hardness test of stainless steel foils as an alternative method for thermal neutron flux monitoring.

2.Material and methods

In the current study, two Am-Be isotopic neutron sources were used. Am activity is 5 Ci/source. The neutron irradiation setup is illustrated schematically in figure (1). Irradiation chamber consists of aluminum tube located between the two Am-Be sources, inside a cylinder of paraffin wax of 58 cm diameter.

High purity Indium and stainless steel foils were used for flux monitoring. Five foils of each type were separated by 1cm of paraffin wax and arranged in a stack as illustrated in figure (1). The stack was separated from the bottom of the irradiation chamber by 10 cm paraffin wax.

The spectra of the emissions of the radioactive samples were measured using a high resolution ORTEC hyper-pure germanium (HPGe) detector of volume 100 cc and efficiency of 70 %. A cylindrical lead-shield of 5 cm thickness, which contains inner concentric thin cylinders of Cu with a thickness of 5 mm, was used to shield the detector and to reduce the effect of background radiation.

Standard gamma sources, of ^{22}Na, ^{60}Co, ^{133}Ba, ^{137}Cs and ^{152}Eu, were used for both energy and efficiency calibrations of the system.

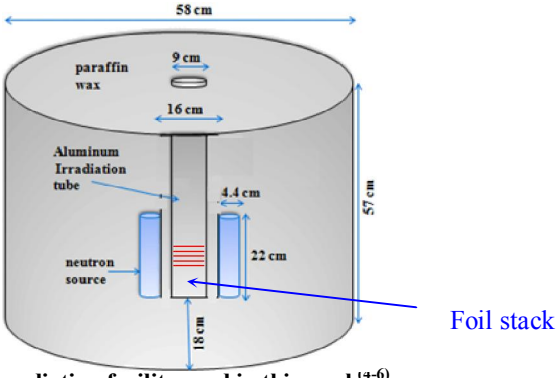

Fig. (1): The layout of Am-Be neutron irradiation facility used in this work[4-6].

The technique used in this work to analyze the stainless steel samples; was Optical Emission Spectrometry (OES).

The optical emission spectrometry (OES) offers a simple, fast, accurate, and precise method for simultaneous determination of multiple trace elements of solid metallic sample [7]. With the help of rotor (1200 revolutions/minute) samples were polished using alumina emery paper of grade 120. OES utilizes a high-energy spark created across an argon-filled gap between an electrode and a sample of the material to be analyzed. A very pure argon gas was used in a flashing mode to isolate the sample from air. The spark creates an emission of radiation from the excited sample surface with wavelengths characteristic of the elemental composition. Two spark stages were used; a pre-spark stage for confirming surface cleaning and a final spark stage for analysis. Different sets of standards were prepared for calibration of the system. The obtained spectrum of radiation is separated into the distinct element-lines and the peak area of each line is measured. The background was taken into account.

Table (1) represents the elemental concentration of five (S1-S5) stainless-steel samples used in this investigation. The major average elements are iron (65-71 %)chromium (12-16%), nickel (7-9%) and other traces.

Table (1): High concentration elementals analysis of used stainless-steel samples using OES.

Element	S1	S2	S3	S4	S5
Fe	69.71	65.29	71.48	66.50	70.30
Cr	15.71	14.71	16.71	12.70	13.70
Ni	8.81	7.86	8.23	9.13	7.83
Ti	1.49	1.32	1.61	1.42	1.83

The hardness tests are roughly classified into three types; the indentation hardness test, the dynamic hardness test and the scratch hardness test. The indentation hardness test is most commonly used today. This test penetrates a permanent deformation of the test piece surface using an indenter of diamond or other rigid body and determines the hardness of the test piece based on the load used to generate the deformation as well as its dimension.

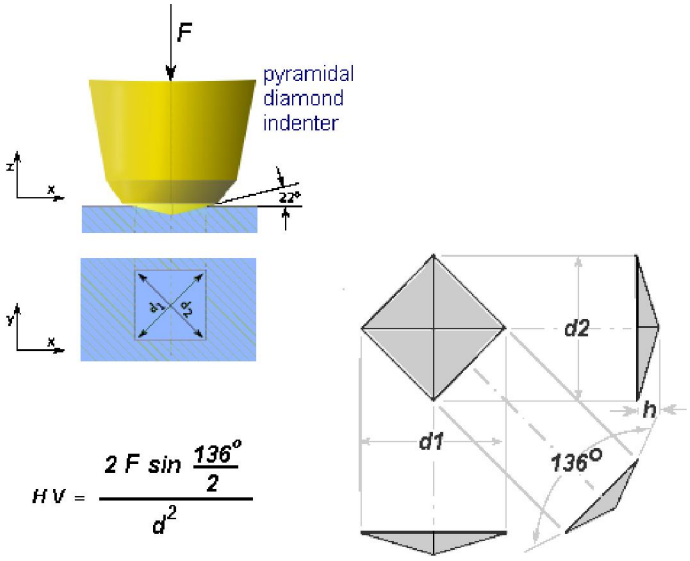

Fig. (2): Vickers hardness test scheme.

The hardness test was performed with the microhardness tester, with capability of performing Vickers hardness test (Figure 2). The Vickers indenter is diamond in the form of a right pyramid with a square base having the angle between the opposite face at the vertex of 136º±30º. The unit of hardness given by the test is known as the Vickers Pyramid Number (HV) or Diamond Pyramid Hardness (DPH). The HV number is determined by the ratio F/A where F is the force applied to the diamond in kilograms-force and A is the surface area of the resulting indentation in square millimeters. The

hardness number then is converted into units of Pascals or Newton/m^2, using hardness conversion table.

The microhardness measurements were carried out using a Schimadzu Microhardness tester with a Vickers diamond pyramid indenter of 136º. The Vickers hardness test was performed on the stainless steel foils in air at room temperature. The indentation were carried out using 2000 gm load at a fixed loading time of 5 seconds for both irradiated and non-irradiated samples. The indentations were made on different locations on the surface for the samples (at least three times for each sample).

The diamond Vickers microhardness is playing a direct practical importance for qualitative and quantitative evaluation of the revealed change of stain steel abrasion resistance and/or scratchability as a result of neutron irradiation.

3.Results and discussion

The gamma spectra of the indium foils (see example spectrum in figure (3)) show a strong and distinct gamma lines of In-116m, which indicates that a reliable flux data can be extracted from such measurements. On the other side Mn-56 exhibits a single and weak gamma line, which indicates that the calculated neutron flux will be not fully reliable with much statistical fluctuation.

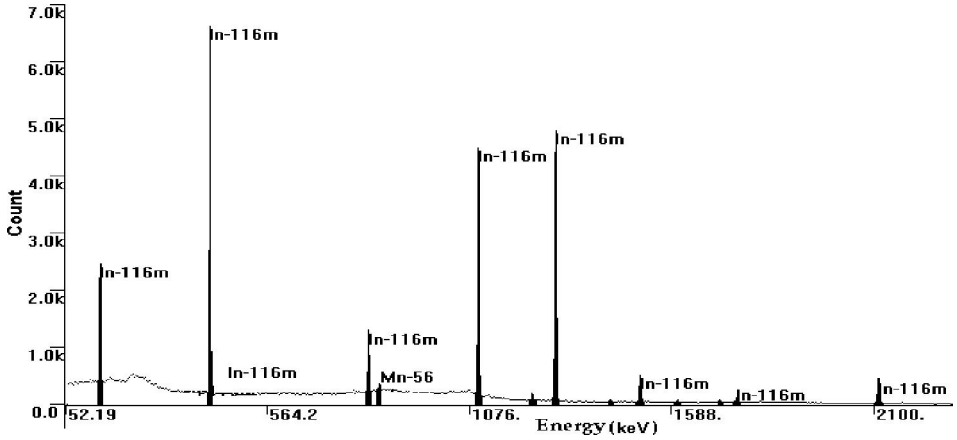

Fig.(3): Gamma spectrum of activated indium foil measured using 70% HPGe.

Figure (4) shows variation of the neutron flux according to the position of monitoring foil in the irradiation chamber as measured by activation of indium and stainless steel foils, through $^{115}In(n,g)^{116m}In$ and $^{55}Mn(n,g)^{56}Mn$ reactions. It reveals that the neutron distribution is not homogenous throughout the irradiation volume.

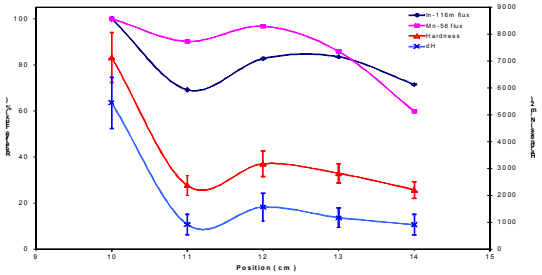

Fig.(4): Represent thermal neutron flux distribution in the irradiation chamber.

Also, figure (4) indicates that the response of ^{115}In and ^{55}Mn is different regarding to the position of the foils. This response is expected owing to the difference in the neutron spectrum throughout the irradiation volume and the cross section dependencies of both isotopes. ^{115}In thermal neutron capture cross section is 202±2 barns, whereas the ^{55}Mn is 13.36±0.1 barns. ^{115}In resonance integral is 3300±100 barns over energy range.0001 to 1 keV, whereas the ^{55}Mn is 14.0±0.3 barns over energy range 0.1 to 100 keV [8]. These data explains the fast drop in the ^{55}Mn measured flux at top positions of the foils, where the neutrons of energy around 100 keV becomes depleted in comparison to neutrons of energy below 1 keV that contributed to the resonance integral of ^{115}In.

In addition, figure (4) shows that the measured hardness of stainless steel foils changes with the position inside irradiation chamber, in a manner corresponding to the neutron flux.

The relation between the change of the measured diamond microhardness and the materials irradiation is represented in figure (5). The relation shows a uniform and gradual increase of hardness with the increase in neutron flux, which can be described by second order polynomial regression. The thermal neutron flux can be calculated through the relation (Figure 6):

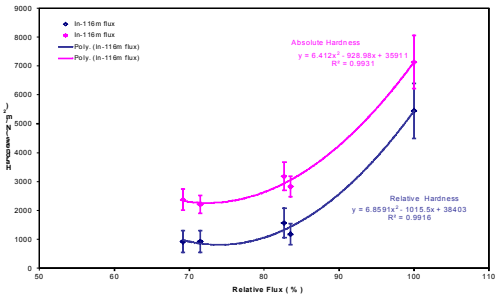

Fig.(5): Represent the relation between the flux and the hardness of stainless steel foils.

$\Phi = A\,(4x10^{-10}\,H^{2} - 8x10^{-6}\,H + 0.0462) / 100$

where Φ in the neutron flux (neutrons/cm^2/s), A is a scaling factor characteristic for the source configuration (in current study = 1.5 X 10^4 neutrons/cm^2/s), H is the Vickers diamond microhardness (Newton/m^2).

Figure (7) presents another alternatives to the Vickers diamond microhardness to flux conversion relations. However, the data based on ^{55}Mn reaction is not fully reliable as discussed before, due to low cross section and the weak gamma line. Therefore, the high fluctuation of ^{55}Mn conversion factor is expected. The data fluctuation is directly affect the goodness of polynomial regression as indicated by the coefficient of determination (R^2). R^2 compares regression and actual values, and ranges from Zero to ONE If it is ONE, there is a perfect correlation. At the other extreme, if the coefficient of determination is ZERO, the regression equation is not helpful in predicting the conversion factor(.[9,10].

Further more for accumulated neutron dose monitoring a foil of S.S were irradiated in the period (1- 7 days). The results can represented by quadratic equation and figure (8), show the trend of this process.

The interaction of neutron beam with stainless steel mainly produces electronic ionization and direct displacement of atoms. Regarding the neutron flux effect on microstructure, the dislocation loop density was reported to increase with increasing neutron flux, and mean diameter had hardly any dependence on neutron flux. The neutron flux dependence of dislocation loop density could be said to be the main factor controlling irradiation hardening under irradiation conditions [11-12]

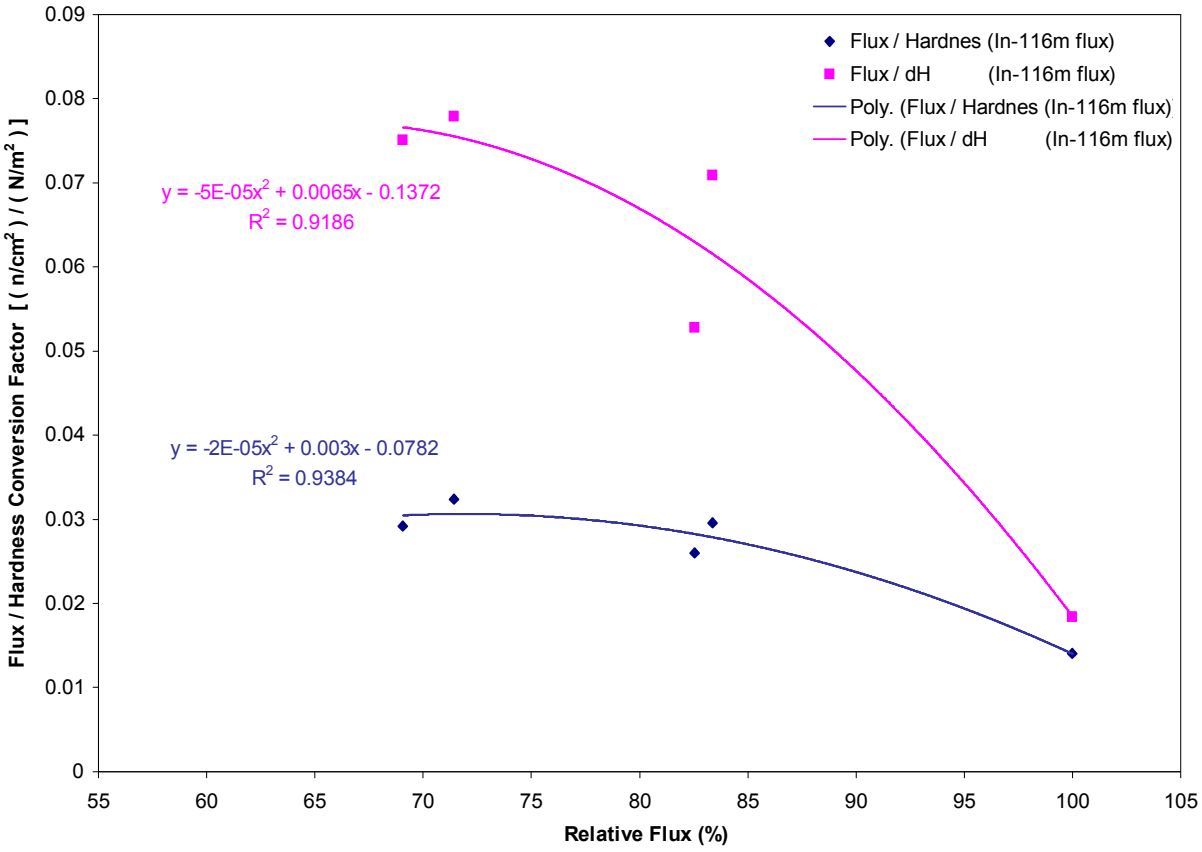

Fig.(6): Represent the stainless steel hardness to flux conversion constant based on the ^{115}In neutron flux.

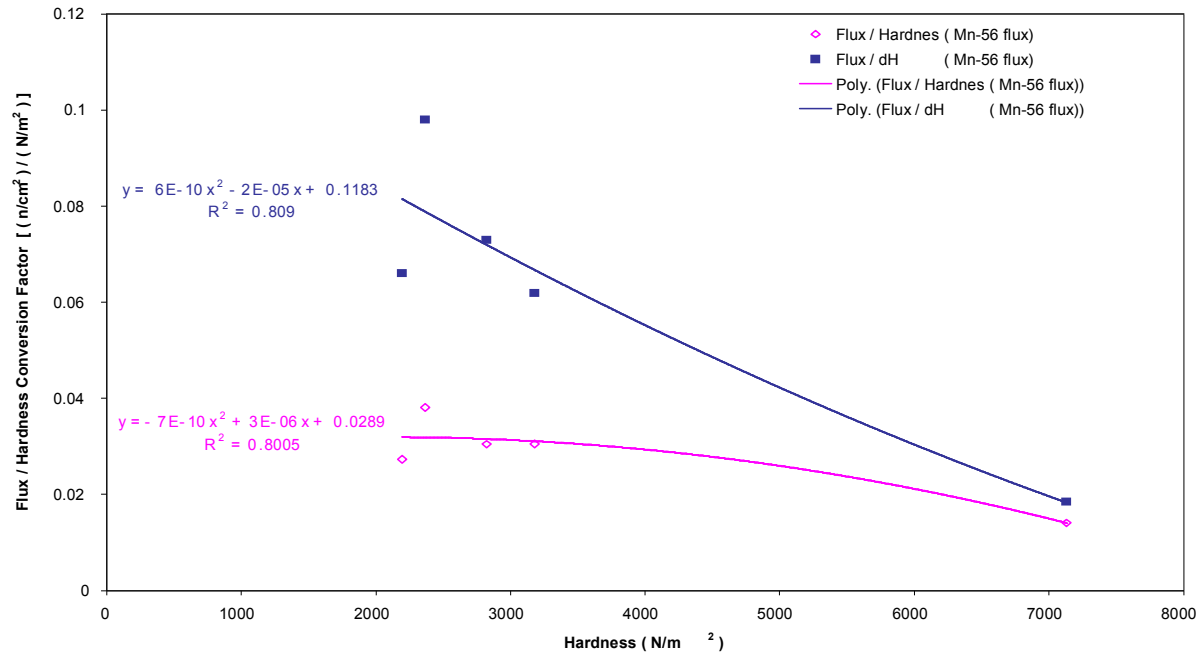

Fig.(7): Represent the stainless steel hardness to flux conversion constant based on the ^{55}Mn neutron flux.

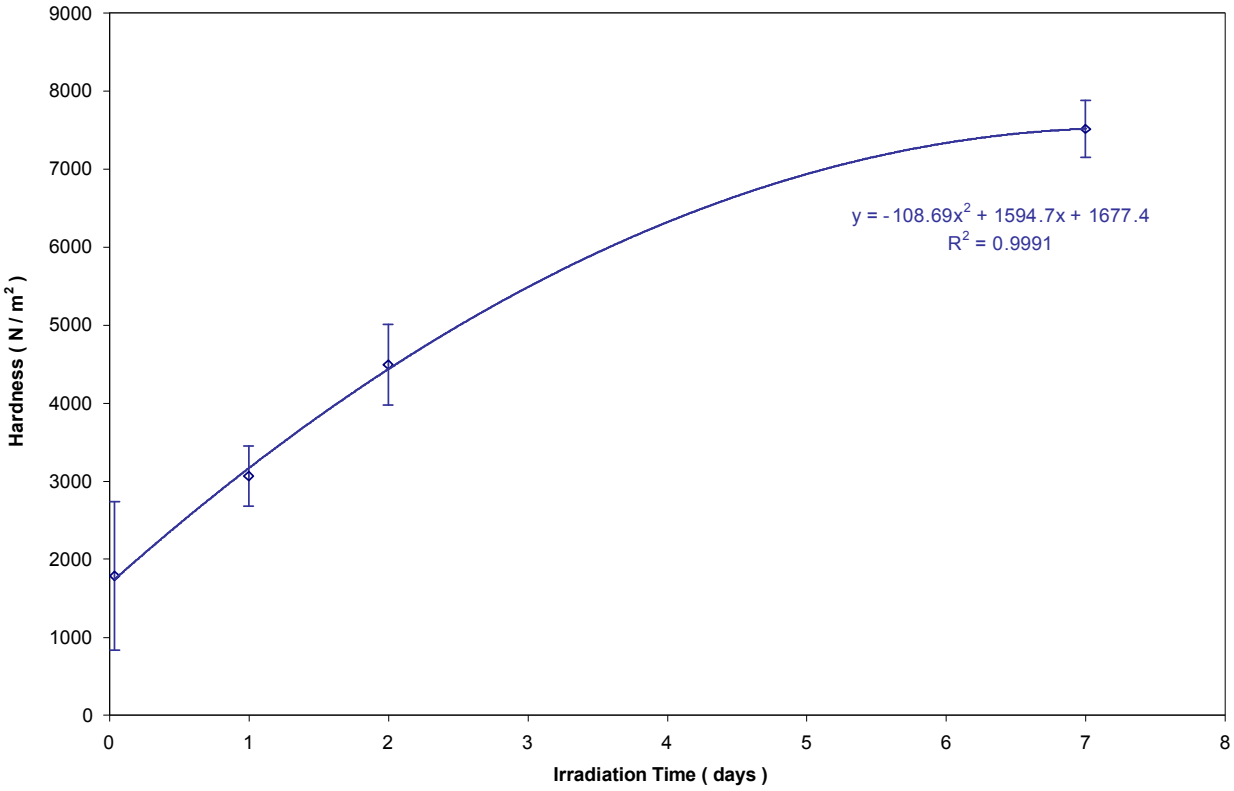

Fig.(8): Represent neutron Flux dependence of hardness increment

Conclusion

The golden goal for this article is to fiend a modern neutron flux monitor method.

The proposed work used a simple off line stress measurement. The proposed tool can well describe the neutron flux intensity at different nuclear reaction positions using thermal neutron gained from Am-Be neutron source. we introduce the method to the field of neutron reactions and neutron therapy to help as accurate, simple, not expensive and safe tool comparing with other technique.

References

(1) ASTM Standard E262–08, "Standard Test Method for Determining Thermal Neutron Reaction Rates and Thermal Neutron Fluence Rates by Radioactivation Techniques" West Conshohocken, PA, March(2009).

(2) ASTM Standard E720–08, "Standard Guide for Selection and Use of Neutron Sensors for Determining Neutron Spectra Employed in Radiation-Hardness Testing of Electronics" West Conshohocken, PA, July(2008).

(3) ASTM Standard E693–01 (Reapproved 2007), "Standard Practice for Characterizing Neutron Exposures in Iron and Low Alloy Steels in Terms of Displacements Per Atom (DPA)" West Conshohocken, PA, July(2007).

(4) Mohamed G.Y., M.Fayez-Hassan, M.Abd-El-Wahab Moustafa Aziz and M.A. Ali, Characteristics of a New Neutron Irradiation Facility Proceeding of 8th Conference on Nuclear and Particle Physics 20-24 Nov. 2o11, Hurghada, Egypt & Arab Journal of Nuclear Sciences and Applications. NUPPAC, 11 TABLE OF CONTENTS on line

(5) Mohamed G.Y., M.Fayez-Hassan, M. Abd El Wahab, Mostafa Aziz and M.A. Ali, Determination of Hydrogen Content for some Egyption Oil Samples using an Am-Be Neutron Source, Journal of Nuclear

Research and Development, NO. 4, Decembre, 2012

(6) M. Bettinelli, G. M. Beone, S. Spezia and C. Baffi; (Determination of heavy metals in soils and sediments by microwave-assisted digestion and inductively couples plasma optical emission spectrometry analysis ….. Analytical Chimica Acta, Vol. 424, Issue 2,289, (2000).

(7) Mughabghab S.F., "Thermal Neutron Capture Cross Sections Resonance Integrals And G-Factors", Iaea Nuclear Data Section, INDC(NDS)-440, February (2003).

(8) Torimaru T., M. Kodama, S. Tanaka, T. Nakamura, and k. Asano, "Neutron Flux Effect on the Irradiation Hardening of Type 304 Stainless Steel", Proceedings of the 22nd Symposium on Effects of Radiation on Materials, held June 8-10,(2004) in Boston.

(9) Gussev M.N., T.S. Byun, and J.T. Busby, "Description of strain hardening behavior in neutron-irradiated fcc metals', Journal of Nuclear Materials 427, 62–68 (2012).

(10) Gold, R.E, and SIM ONEN, E.P., Eds. Radiation harding effects on localised deformation and stress corrosion cracking of stainless steel, The minerals, material socity wavrenelale, Pennsylvania, (1993) 537

(11) Gross beck M.L., T.R. Allen and A.S kumar, Eds., Hardness and Mictostructure changes with thermal annealing of irradiated Fe – Cu alloys. American Society for Testing and Materials West. PA, (2000).

2013/12/3